Quantum steerability of two qubits mediated by one-dimensional plasmonic waveguides

Ye-Qi Zhang(张业奇)[1], Xiao-Ting Ding(丁潇婷)[1], Jiao Sun(孙娇)[1], and Tian-Hu Wang(王天虎)[2,†]

[1] *Department of Mathematics and Physics, North China Electric Power University, Beijing* 102206, *China*
[2] *School of Energy Power and Mechanical Engineering, North China Electric Power University, Beijing* 102206, *China*

(Received 28 June 2022; revised manuscript received 1 August 2022; accepted manuscript online 19 August 2022)

We study the dynamics of the quantum steering between two separated qubits trapped in a one-dimensional plasmonic waveguide. By numerical methods, we calculate the quantum steerability and other quantum correlations, i.e., entanglement, discord, and coherence, for both cases with and without laser driving fields. It is found that steerability may exhibit a sudden disappearance and sudden reappearance phenomenon. Specifically, there exist time windows with no steerability but finite entanglement. The effects of plasmon wavenumber and the distance between the two qubits on steerability are also examined. Furthermore, we show that quantum steerability is tunable by adjusting the laser driving fields.

Keywords: quantum steering, quantum correlations, plasmonic waveguide

PACS: 03.65.Ud, 03.67.–a, 73.20.Mf **DOI:** 10.1088/1674-1056/ac8af8

1. Introduction

Steering, firstly proposed by Schrödinger,[1] is a quantum effect that a distant part can remotely prepare ensembles of quantum states by performing local measurements with the aid of entanglement. It allows one to certify the presence of entanglement between a device-untrusted part and a device-trusted part.[2,3] Due to the fact that certification of entanglement[4] requires quantum measurements on both sides, whereas in Bell nonlocality,[5] both parts possess untrusted black-box devices, steering can be treated as a type of quantum correlation situating between entanglement and Bell nonlocality. Several experiments,[6–10] including steering without Bell nonlocality[11] and a fully loop-hole free steering demonstration,[12] have verified the steering phenomenon. Like entanglement, quantum steering has been regarded as a quantum resource.[13] It plays an important role in the one-sided device-independent quantum key distribution (1S-DI-QKD), where only one of the parts has an untrusted device while the other ones possess the trusted apparatus.[14,15] The 1S-DI-QKD has the advantage that its experimental requirements for unconditionally secure keys are less rigorous than those in both-sided DI-QKD.[16] Besides, it is found recently that quantum steering can also be used to demonstrate network steering[17] and can be observed on IBM quantum computers.[18]

On the other hand, the realization of establishing long-distance nonclassical correlations (between two nodes of a quantum network), especially in dissipative environments, is crucial for quantum information processing.[19] It has been reported that photons can be used as a medium to set up entanglement between two qubits.[20,21] Meanwhile, several proposals for mediating long-distance quantum correlations of two nodes by using plasmons have attracted considerable interest.[22–29] Plasmons traveling along a surface are known as surface plasmon polaritons which can be typically excited by light waves striking on a metal surface.[30] Since plasmons display a strong local surface effect, it is effective for breaking the classical diffraction limit and manipulating light in the nanoscale domain. It was shown that the spontaneous formation of a high degree of entanglement can be acquired, even for the separation of subsystems are larger than the operating wavelength.[31] With the development of nanotechnologies, strong and efficient coupling in plasmonic quantum electrodynamics is attainable and plasmons become a possible candidate for quantum information science.[32–35]

In this paper, we investigate the dynamics of quantum steering between two separated qubits which are modulated by a one-dimensional plasmonic waveguide. Staring from the master equation that governs the dissipative dynamics of the two qubits for arbitrary initial states, we numerically calculate the quantum steerability using the semidefinite program. It is shown that the dynamical behavior is largely dependent on the plasmon wavenumber and the distance between the two qubits. By comparing with quantum entanglement, discord and coherence, we find quantum steerability is more fragile under dissipative environments. In particular, steerability would undergo sudden disappearance and sudden reappearance processes. It is found that there exist time windows with zero steerability but finite entanglement for the system. The features of fixed and random direction measurement protocols on steerability are also examined. In order to tune the dynamical behavior of steerability, classical fields for driving could be locally applied

†Corresponding author. E-mail: thwang@ncepu.edu.cn
© 2022 Chinese Physical Society and IOP Publishing Ltd

to the qubits. We demonstrate that under continuous driving, time duration with finite steerability can be enlarged remarkably.

2. Two qubits mediated by a one-dimensional plasmonic waveguide

In this paper, we consider identical qubits trapped in a V-shaped one-dimensional plasmonic waveguide (1D-PW). Usually, surface plasmon polaritons dissipate due to the internal losses in the metal and the radiation losses. Hence, waveguides are needed to confine and direct the propagation of surface plasmon polaritons with minimal energy loss.[36] Metallic structured waveguides can display strong field concentration and it has been shown that a one-dimensional V-shaped channel is more efficient for establishing entanglement than a cylinder nanowire.[31] Moreover, the V-shaped waveguide stands out as a competitive structure as it can promote a large coupling efficiency β due to the strong EM confinement it offers.[37] The V-shaped 1D-PW has a V-groove structure that is milled on a silver film. As shown in Fig. 1, the two qubits are placed symmetrically along the direction of the plasmonic waveguide with a distance of d. To ensure that the two qubits are equally influenced by the 1D-PW, their vertical distances from the surface are all set to be h. With considering the spontaneous emission of qubits, the dynamic density matrix ρ of two qubits can be obtained by the following master equation:[38,39]

$$\partial_t \rho = \frac{\mathrm{i}}{\hbar}[\rho, H] + \sum_{i,j=1,2} \frac{\gamma_{ij}}{2}(2\sigma_i \rho \sigma_j^\dagger - \sigma_i^\dagger \sigma_j \rho - \rho \sigma_i^\dagger \sigma_j), \quad (1)$$

where $\sigma_i^\dagger$ and σ_i are the raising and lowering operators of the ith qubit, respectively. In Eq. (1), the first term is the incoherent term, and the second term is the coherent term, which describes the effective interaction between two qubits. The decay rate of a single qubit is γ_{11} (γ_{22}), and the cross-decay rate of two qubits is γ_{12} (γ_{21}). To simplify, we assume that $\gamma_{11} = \gamma_{22} \equiv \gamma$ and $\gamma_{12} = \gamma_{21}$. For two qubits with the same characteristic frequency ω_0, the Hamiltonian can be written as follows:

$$H = \hbar\omega_0 \sum_{i=1,2} \sigma_i^\dagger \sigma_i + g_{12}(\sigma_1^\dagger \sigma_2 + \sigma_2^\dagger \sigma_1), \quad (2)$$

where coherent dipole–dipole coupling rate is expressed by g_{12}. It was found that when the propagating plasmon is the main channel of emission (i.e., the large β factor, which represents the fraction of emitted radiation captured by the propagation model), a good approximation of the total Green's function can be obtained.[40] In this way, the analytical expressions of g_{12} and γ_{12} can be derived

$$g_{12} = \frac{\gamma}{2}\beta \mathrm{e}^{-d/(2L)} \sin(k_{\mathrm{pl}} d),$$

$$\gamma_{12} = \gamma\beta \mathrm{e}^{-d/(2L)} \cos(k_{\mathrm{pl}} d), \quad (3)$$

where k_{pl} and L are the wavenumber and propagation length of plasmon, respectively. k_{pl} is related to the mode wavelength λ_{pl} of the plasmon, that is, $k_{\mathrm{pl}} \cdot \lambda_{\mathrm{pl}} = 2\pi$. The key point of Eq. (3) is that the $\pi/2$ phase shifts between coherent and incoherent phases of coupling. As we will see below, it can change one of the two contributions and maximize the other contribution by adjusting the distance between the qubits, thus opening the possibility of modulating the degree of quantum correlations.

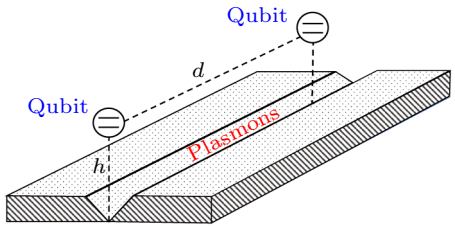


Fig. 1. Schematic diagram of the interaction between a two-qubit system and a one-dimensional plasmonic waveguide with V-shaped structure.

The general form of density matrix for two quantum element systems is

$$\rho(t) = \begin{pmatrix} \rho_1(t) & \rho_2(t) & \rho_3(t) & \rho_4(t) \\ \rho_2^*(t) & \rho_5(t) & \rho_6(t) & \rho_7(t) \\ \rho_3^*(t) & \rho_6^*(t) & \rho_8(t) & \rho_9(t) \\ \rho_4^*(t) & \rho_7^*(t) & \rho_9^*(t) & \rho_{10}(t) \end{pmatrix}, \quad (4)$$

which satisfies $\rho_1 + \rho_5 + \rho_8 + \rho_{10} = 1$. The dynamics matrix is written in the basis $|1\rangle = |g_1, g_2\rangle$, $|2\rangle = |g_1, e_2\rangle$, $|3\rangle = |e_1, g_2\rangle$, and $|4\rangle = |e_1, e_2\rangle$. Substituting Eq. (4) into Eq. (1), we obtain the differential equations for the non-zero elements of the density matrix as follows:

$$\begin{aligned}
\dot{\rho}_1(t) &= \gamma(\rho_5(t) + \rho_8(t)) + \gamma_{12}(\rho_6(t) + \rho_6^*(t)), \\
\dot{\rho}_2(t) &= \frac{\gamma}{2}(2\rho_9(t) - \rho_2(t)) + \frac{\gamma_{12}}{2}(2\rho_7(t) - \rho_3(t)) \\
&\quad + \mathrm{i}g_{12}\rho_3(t), \\
\dot{\rho}_3(t) &= \frac{\gamma}{2}(2\rho_7(t) - \rho_3(t)) + \frac{\gamma_{12}}{2}(2\rho_9(t) - \rho_2(t)) \\
&\quad + \mathrm{i}g_{12}\rho_2(t), \\
\dot{\rho}_4(t) &= -\gamma\rho_4(t), \\
\dot{\rho}_5(t) &= \gamma(\rho_{10}(t) - \rho_5(t)) - \frac{\gamma_{12}}{2}(\rho_6(t) + \rho_6^*(t)) \\
&\quad + \mathrm{i}g_{12}(\rho_6(t) - \rho_6^*(t)), \\
\dot{\rho}_6(t) &= \frac{\gamma_{12}}{2}(2\rho_{10}(t) - \rho_5(t) - \rho_8(t)) - \gamma\rho_6(t) \\
&\quad + \mathrm{i}g_{12}(\rho_5(t) - \rho_8(t)), \\
\dot{\rho}_7(t) &= -\frac{1}{2}(3\gamma\rho_7(t) + (2\mathrm{i}g_{12} + \gamma_{12})\rho_9(t)), \\
\dot{\rho}_8(t) &= \gamma(\rho_{10}(t) - \rho_8(t)) - \frac{\gamma_{12}}{2}(\rho_6(t) + \rho_6^*(t)) \\
&\quad - \mathrm{i}g_{12}(\rho_6(t) - \rho_6^*(t)),
\end{aligned}$$

$$\dot{\rho}_9(t) = -\left(\mathrm{i}g_{12} + \frac{\gamma_{12}}{2}\right)\rho_7(t) - \frac{3}{2}\gamma\rho_9(t),$$
$$\dot{\rho}_{10}(t) = -2\gamma\rho_{10}(t). \tag{5}$$

3. Quantum steering and other correlations

If an entangled state is shared by a bipartite system, one side performs local measurements on one subsystem, then different results will cause different states on the other remote subsystem. This phenomenon is called quantum steering. Let us consider two parts, possessed by Alice and Bob, where Alice wants to convince Bob that they share an entanglement state. Alice would perform one measurement from a set of m choices, each of which has n possible outcomes. After she obtains the outcome, Alice will send the result to Bob. On the other hand, Bob has a trusted device and can make a full state tomography to obtain an accurate quantum description of his system. According to the results from Alice and the conditioned state on his own, Bob can tell whether they hold an entanglement or not.

A steering experiment therefore can be fully characterized by giving an assemblage $\{\sigma_{a|x}\}_{ax}$, which is a set of non-normalized states Alice steers Bob into, given her choice of measurement x and the corresponding outcome a. The assemblage encodes the conditional probability distribution of the Alice result from the given input, $p(a|x) = \mathrm{Tr}(\sigma_{a|x})$, and the conditional state for Bob $\hat{\sigma}_{a|x} = \sigma_{a|x}/P(a|x)$. All valid assemblages meet consistency requirements

$$\sum_a \sigma_{a|x} = \sum_a \sigma_{a|x'}, \quad \forall x, x',$$
$$\mathrm{Tr}\sum_a \sigma_{a|x} = 1, \quad \forall x. \tag{6}$$

It reveals the fact that Alice cannot signal to Bob, and without Alice's information, Bob still has a valid quantum state. Quantum steering is formally defined by Jones *et al.*[41] as the possibility of remotely generating ensembles that could not be produced by a local hidden state model. All the unnormalized states in an assemblage can be written in the form

$$\sigma_{a|x} = \sum_\lambda D_\lambda(a|x)\sigma_\lambda, \quad \forall x, a,$$
$$\text{with } \mathrm{Tr}\sum_\lambda \sigma_\lambda = 1, \quad \sigma_\lambda \geq 0, \quad \forall\lambda, \tag{7}$$

where λ is the classical random variable held by Alice, $D_\lambda(a|x)$ are deterministic single party conditional probability distributions for Alice, and σ_λ is the state held by Bob. We call such an assemblage unsteerable and the set of unsteerable assemblages is represented by Σ^{US}. Any assemblages that cannot be written in Eq. (7) constitutes a genuine resource in a steering scenario and is called steerable. The set of steerable assemblage is represented by Σ^{S}. Using the semidefinite program (SDP),[42] we can test whether a given assemblage is in a set of unsteerable assemblage, i.e., if $\{\sigma_{a|x}\}_{ax} \in \Sigma^{\mathrm{US}}$.

Here, we adopt the steerable weight (SW) introduced by Skrzypczyk *et al.*[43] as a measure of steerability for a bipartite state. The main ideas behind the SW are as follows. When preparing a given assemblage, Alice should reduce the number of uses of real steering resources and prepare as frequently as possible an unsteerable assemblage. In other words, we decompose the assemblage into

$$\sigma_{a|x} = \mu\sigma^{\mathrm{US}}_{a|x} + (1-\mu)\sigma^{\mathrm{S}}_{a|x}, \quad \forall a, x, \quad 0 \leq \mu \leq 1, \tag{8}$$

where $\{\sigma^{\mathrm{US}}_{a|x}\}$ is the unsteerable part, and $\{\sigma^{\mathrm{S}}_{a|x}\}$ is the steerable part. The SW is naturally defined as the minimal amount of genuine steerable resource to reproduce this assemblage. Mathematically, $\mathrm{SW} = 1 - \mu^*$ where μ^* is the maximum of μ and can be obtained from SDP

$$\begin{aligned} &\max\ \mathrm{Tr}\sum_\lambda \sigma_\lambda, \\ &\text{s.t. } \sigma_{a|x} - \sum_\lambda D_\lambda(a|x)\sigma_\lambda \geq 0, \quad \forall x, a, \\ &\sigma_\lambda \geq 0, \quad \forall\lambda. \end{aligned} \tag{9}$$

As comparative quantum correlations, to explore the significant properties of quantum steering in studying the plasmonic waveguide model, we calculate the entanglement, quantum discord, and coherence as comparative quantities. They have been widely used to measure quantum correlations in other systems. Here we briefly introduce their definitions. Concurrence,[44] as a measure of quantum entanglement, for two-qubit states, the following results can be obtained:

$$C(\rho) = \max\left\{0, \sqrt{\Lambda_1} - \sqrt{\Lambda_2} - \sqrt{\Lambda_3} - \sqrt{\Lambda_4}\right\}, \tag{10}$$

where Λ_i's are four eigenvalues of the following matrix in decreasing order $\rho(\sigma_y \otimes \sigma_y)\rho^*(\sigma_y \otimes \sigma_y)$, where ρ^* is the complex conjugate of the density matrix ρ and σ_y is the Pauli Y operator.

Quantum discord[45] of a state ρ is defined as the difference between the quantum mutual information $M(\rho)$ and classical correlation $CC(\rho)$

$$D(\rho) = M(\rho) - CC(\rho), \tag{11}$$

where $M(\rho) = S(\rho_A) + S(\rho_B) - S(\rho)$, ρ_A (ρ_B) is the reduced density matrix of subsystem A (B) of the compound bipartite system AB, and $S(\rho)$ is the von Neumann entropy $S(\rho) = -\mathrm{tr}\rho\log_2\rho$. The classical correlations can be defined by using Von Neumann type measurements. Consider a complete set of orthogonal projectors $\{B_j\}$ to describe the projection measurements only acts on system B. The condition matrix associated with the measurement result j is $\rho_j = (\mathbb{1}\otimes\{B_j\})\rho(\mathbb{1}\otimes\{B_j\})$, where $\mathbb{1}$ is the identity matrix of subsystem A and the probability of obtaining the measurement result j is $p_j = \mathrm{tr}[(\mathbb{1}\otimes\{B_j\})\rho(\mathbb{1}\otimes\{B_j\})]$. The total classical correlations are defined as the following superior limit $CC(\rho) = S(\rho_A) - \min_{\{B_j\}}\sum_j p_j S(\rho_j)$.

Another useful quantum resource is the coherence and we adopt the relative entropy of coherence[46] as the measure for the state ρ

$$C_{\mathrm{R}}(\rho) = S(\rho_{\mathrm{diag}}) - S(\rho), \tag{12}$$

where ρ_{diag} denotes the state obtained from ρ by deleting all off-diagonal elements. Moreover, we may also consider the purity $\mathrm{tr}(\rho^2)$ of the state ρ.

4. Results and discussion

Now, we draw on the master equation to analyze the time-dependent behavior of quantum steerability. We employ the numerical approach to calculate the density matrix at any time and the SW for both cases with and without laser drivings. In order to obtain the SW, one must choose the set of measurement choices beforehand. Here, we adopt $m = 3$ and study two measurement strategies. One is the fixed 3 directions of σ_x, σ_y, σ_z and the other is to maximize over 1000 randomly generated 3 direction measurements.

We plot the SW, concurrence, quantum discord, coherence and purity as functions of the dimensionless time γt with $\bar{\beta} = 0.9$, $k_{\mathrm{pl}}d = 2\pi$ for initial states $|e_1, g_2\rangle$ in Fig. 2(a). We can see that at the very beginning, the SW increases abruptly. This is because the phenomenon of quantum steering is based on entanglement but they are not completely equivalent. The initial state $|e_1, g_2\rangle$ is a separable state containing no entanglement so that it cannot has SW. And we can see that as the state becomes weakly entangled but with large purity, the SW becomes very strong. In fact, a pure state has maximal steerability, no matter how weak entanglement it contains.[47,48] Hence, states with small entanglement but high purity may have large steerability. Then the SW decreases quickly and disappears suddenly. This phenomenon is similar to the sudden death of entanglement.[49] The behaviors of concurrence, discord, and coherence are quite different. As the SW decreases, all concurrence, discord, and coherence increase firstly, reach the maximum points, then disappear gradually. We can see from the figure that there exists entanglement which is useless for quantum steering, hence the dynamics of steering and entanglement are quite different.

In Fig. 2(b), we plot the evolution of the largest SW over 1000 randomly generated 3 direction measurements as a function of dimensionless time γt with $\bar{\beta} = 0.9$ and $k_{\mathrm{pl}}d = 2\pi$ for initial state $|e_1, g_2\rangle$. Compared with Fig. 2(a), we can see that the evolution behaviors of SW for fixed and random measurement strategies are similar. It suggests that fixed measurements on σ_x, σ_y, and σ_z are also enough to exploit our system for quantum steering. Moreover, the distributions of SW are given in the insets for some moments. It shows that, as the value of SW increases, the distribution of SW becomes increasingly peaked around the maximum value.

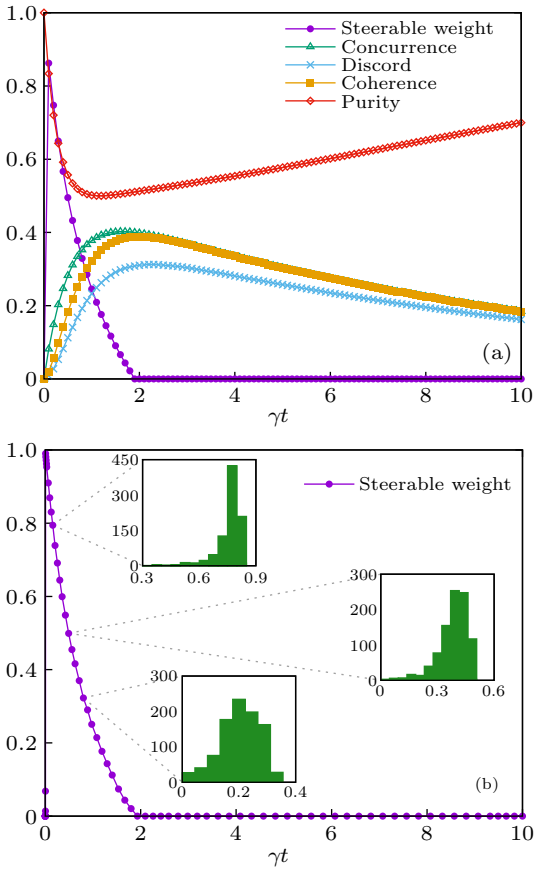


Fig. 2. (a) The SW, concurrence, quantum discord, coherence and purity as functions of dimensionless time γt, with fixed measurement strategy. (b) The SW as a function of dimensionless time γt, with random measurement strategy. For both panels, the initial state is $|e_1, g_2\rangle$, $\bar{\beta} = \beta \mathrm{e}^{-d/(2L)} = 0.9$, $k_{\mathrm{pl}}d = 2\pi$. Insets of panel (b): the population distributions of SW over the ensemble of assemblages.

In the following, we consider the scheme of tuning quantum steerability by locally applying two classical fields. Under the condition of continuous drivings, a new term $\sum_{i=1,2} \Omega_i(\sigma_i^{\dagger} + \sigma_i)$ should be added to the effective Hamiltonian given in Eq. (2), where Ω_i is the coupling strength between the i-th qubit and its classical field with frequency ω_{c}. Here, we consider three different driving conditions: (i) asymmetric driving ($\Omega_1 \neq 0$, $\Omega_2 = 0$); (ii) antisymmetric driving ($\Omega_1 = -\Omega_2 \neq 0$) and (iii) symmetric driving ($\Omega_1 = \Omega_2 \neq 0$). For simplicity, we consider the same initial state $|e_1, e_2\rangle$ and $\bar{\beta} = 0.99$ in all below cases.

We plot the SW, concurrence, quantum discord, coherence, and purity as functions of the dimensionless time γt in Fig. 3(a) with $\Omega_1 = 0.15\gamma$, $\Omega_2 = 0$, and $k_{\mathrm{pl}}d = \pi$. At the very beginning, similar to Fig. 2(a), the SW increases abruptly from zero. The SW firstly increases and then suddenly disappears, while concurrence, discord, coherence, and purity maintain oscillating. We can see from the figure that there exist time windows with no steerability but finite entanglement, which should be avoided performing operations using steering. In the following, the SW will suddenly reappear for a time interval, in which the system could be used for steering again. This sudden disappearance and reappearance phenomenon only occurs

twice in evolution. All other quantities will maintain steady at some values. In Fig. 3(b), we plot the evolution of the biggest SW over 1000 randomly generated 3 direction measurements as a function of γt with $\Omega_1 = 0.15\gamma$, $\Omega_2 = 0$, and $k_{\rm pl}d = \pi$. Compared with Fig. 3(a), we can see that the behavior of SW obtained by random measurements is consistent with that using fixed measurements. In the remaining paper, we will only consider fixed measurements. The distribution of SW is also given in the insets. It reveals the fact again that the bigger value of SW, the closer to the maximum value that the distribution of SW peaked.

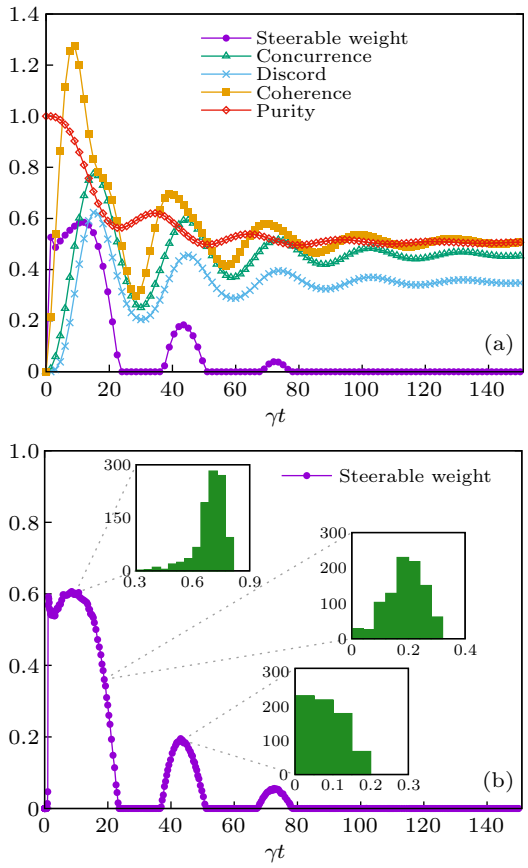


Fig. 3. (a) The SW, concurrence, quantum discord, coherence and purity as functions of dimensionless time γt, with fixed measurement strategy. (b) The SW as a function of dimensionless time γt, with random measurement strategy. For both panels, the initial state is $|e_1, g_2\rangle$, $\bar{\beta} = \beta e^{-d/(2L)} = 0.99$, $k_{\rm pl}d = \pi$, $\Omega_1 = 0.15\gamma$, $\Omega_2 = 0$. Insets of panel (b): the distribution of SW over the ensemble of assemblages.

In Fig. 4(a), we plot the SW, concurrence, quantum discord, coherence and purity as functions of the γt with $\Omega_1 = 0.3\gamma$, $\Omega_2 = -0.3\gamma$, and $k_{\rm pl}d = \pi$. Compare with Fig. 2(a), we can see that the evolution behaviors with antisymmetric driving are different from those without classical driving. Due to the effects of classical fields, the time duration with finite steerability is much longer than that without driving. In Fig. 4(b), we plot same quantities as functions of the γt with $\Omega_1 = \Omega_2 = 0.15\gamma$ and $k_{\rm pl}d = \pi$. We observe that the SW firstly gradually increases to the maximum and then decays to disappear. After a while, it suddenly reappears then vanishes again. All other quantities would oscillate before reaching a steady value. Compared with Fig. 3(a), we can see the oscillation frequency with symmetric driving is faster than that with asymmetric driving. In order to see the effects of coherent and incoherent phases of coupling, we plot the SW as a function of γt, with $\Omega_1 = \Omega_2 = 0.2\gamma$, for both $k_{\rm pl}d = \pi$ and $k_{\rm pl}d = 2\pi$ in Fig. 5. It is shown that when $k_{\rm pl}d = 2\pi$, the SW firstly increases to the maximum and then decays asymptotically to zero, while for $k_{\rm pl}d = \pi$, the SW would exhibit sudden disappearance and reappearance phenomenon. By comparison, we find that for symmetric driving, the SW maintains for a longer time at $k_{\rm pl}d = 2\pi$, which is beneficial for executing quantum processing tasks by using quantum steering.

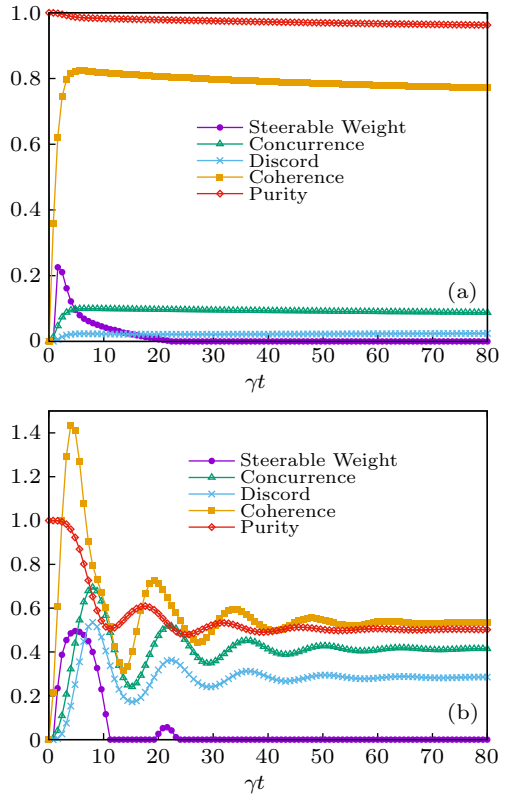


Fig. 4. The SW, concurrence, quantum discord, coherence and purity as functions of dimensionless time γt with $\bar{\beta} = \beta e^{-d/(2L)} = 0.99$, $k_{\rm pl}d = \pi$, (a) $\Omega_1 = 0.3\gamma$ and $\Omega_2 = -0.3\gamma$, (b) $\Omega_1 = 0.15\gamma$ and $\Omega_2 = 0.15\gamma$.

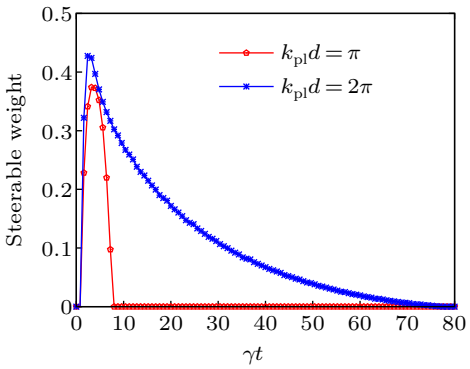


Fig. 5. The SW as a function of dimensionless time γt for two different values of the product $k_{\rm pl}d$ with $\bar{\beta} = \beta e^{-d/(2L)} = 0.99$, $\Omega_1 = 0.2\gamma$, $\Omega_2 = 0.2\gamma$. The dash represents $k_{\rm pl}d = 2\pi$, the solid represents $k_{\rm pl}d = \pi$.

Finally, in order to see more clearly the difference between dynamical behaviors of steering and entanglement in our model, we plot the SW and concurrence as functions of γt and $k_{\rm pl}d$ with $\Omega_1 = 0.15\gamma$, $\Omega_2 = 0$ in Figs. 6(a) and 6(b), respectively. We can see from the figures that, at any given time, both SW and concurrence are periodically oscillating along $k_{\rm pl}d$ with the period π. The maximum values would be obtained at $n\pi$, where n is an integer. As γt increases, the SW will vanish eventually for all values of $k_{\rm pl}d$. We can see clearly that vast regions have finite entanglement but zero steerability, which suggests one should be more elaborate when exploiting quantum steering, for it is more difficult to be established and maintained than entanglement. In fact, there is a strict inclusion relation between entanglement, steering, and violation of a Bell inequality in the sense that there are entangled states that cannot be used for steering, and there are steerable states that do not violate any Bell inequality.[50]

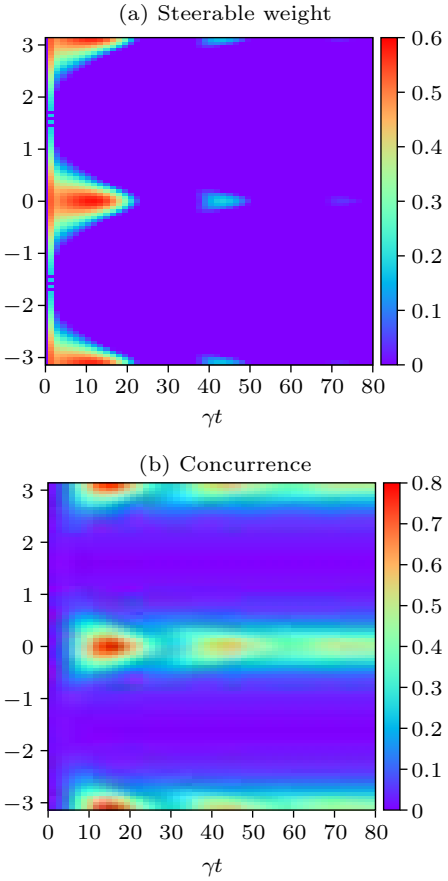


Fig. 6. The SW (a) and concurrence (b) as a function of the dimensionless time γt and the product $k_{\rm pl}d$ is displayed with $\tilde{\beta} = \beta e^{-d/(2L)} = 0.99$, $\Omega_1 = 0.15\gamma$, $\Omega_2 = 0$.

5. Conclusion

In summary, we have studied the dynamics of quantum steering between two separated qubits which are modulated by a one-dimensional plasmonic waveguide. By semidefinite program, we numerically solve the master equation and obtain the dynamics of quantum steerability for the two-qubit system. We show that the dynamical behavior strongly depends on the plasmon wavenumber and the distance between the two qubits. It is worth noting that the maximum quantum steerability can be achieved if the value of the product $k_{\rm pl}d$ is selected to be around $n\pi$ for integers n. Quite different from entanglement, discord, and coherence, the phenomenon of sudden disappearance and reappearance occurs in the dynamics of steerability. We find that, under dissipative environments, quantum steerability is more fragile than other quantum correlations. To utilize steering, one needs to avoid time windows in which the system has zero steerability but finite entanglement. We have also examined the features of fixed and random direction measurements. Finally, the tuning effect of the classical driving fields on the system is discussed. It is shown that, under continuous driving, time duration with finite steerability can be remarkably enlarged. We show that plasmon polaritons in one-dimensional waveguides are excellent candidates as mediators for establishing steerability between two distant qubits. Our results may have potential benefits in designing nanoscale devices for quantum information processing tasks such as 1S-DI-QKD.

Acknowledgments

Project supported by the National Natural Science Foundation of China (Grant Nos. 51876059 and 11805065) and the Fundamental Research Funds for the Central Universities (Grant Nos. 2021MS009 and 2021MS046).

References

[1] Schrödinger E and Born M 1935 *Proc. Cambridge Philos. Soc.* **31** 555
[2] Wiseman H M, Jones S J and Doherty A C 2007 *Phys. Rev. Lett.* **98** 140402
[3] Reid M D, Drummond P D, Bowen W P, Cavalcanti E G, Lam, P K, Bachor H A, Andersen U L and Leuchs G 2009 *Rev. Mod. Phys.* **81** 1727
[4] Horodecki R, Horodecki P, Horodecki M and Horodecki K 2009 *Rev. Mod. Phys.* **81** 865
[5] Brunner N, Cavalcanti D, Pironio S, Scarani V and Wehner S 2014 *Rev. Mod. Phys.* **86** 419
[6] Smith D H, Gillett G, Almeida M P D, Branciard C and White A G 2012 *Nat. Commun.* **3** 625
[7] Wollmann S, Uola R and Costa A C S 2020 *Phys. Rev. Lett.* **125** 020404
[8] Huang C Y, Xiang G Y, Guo Y, Wu K D, Liu B H, Li C F, Guo G C and Tavakoli A 2021 *Phys. Rev. Lett.* **127** 020401
[9] Liu S, Han D, Wang N, Xiang Y, Sun F, Wang M, Qing Z, Gong Q, Sun X and He Q 2022 *Phys. Rev. Lett.* **128** 200401
[10] Shi J, He X, Chen W, Li Y, Kang M, Cai Y and Xu H 2022 *Nano Lett.* **22** 688
[11] Saunders D J, Jones S J, Wiseman H M and Pryde G J 2010 *Nat. Phys.* **7** 918
[12] Wittmann B, Ramelow S, Steinlechner F, Langford N K, Brunner N, Wiseman H M, Ursin R and Zeilinger A 2012 *New J. Phys.* **14** 053030
[13] Gallego R and Aolita L 2015 *Phys. Rev. X* **5** 041008
[14] Branciard C, Cavalcanti E G, Walborn S P, Scarani V and Wiseman H M 2012 *Phys. Rev. A* **85** 010301
[15] Xin J, Lu X M, Li X and Li G 2020 *Opt. Exp.* **28** 11439
[16] Acín A, Brunner N, Gisin N, Massar S, Pironio S and Scarani V 2007 *Phys. Rev. Lett.* **98** 230501
[17] Jones B D M, Supic I, Uola R, Brunner N and Skrzypczyk P 2021 *Phys. Rev. Lett.* **127** 170405

[18] Seifert L M, Beyer K, Luoma K and Strunz W T 2022 *Phys. Rev. A* **105** 042413

[19] Kimble H J 2008 *Nature* **453** 1023

[20] Yan Z H, Qin J L, Qin Z Z, Su X L, Jia X J, Xie C D and Peng K C 2021 *Fundament. Res.* **1** 43

[21] Arauújo M O, Marinlo L S and Felinto D 2022 *Phys. Rev. Lett.* **128** 083601

[22] Gonzalez-Tudela A, Martin-Cano D, Moreno E, Martin-Moreno L, Tejedor C and Garcia-Vidal F J 2011 *Phys. Rev. Lett.* **106** 020501

[23] Zheng H and Baranger H U 2013 *Phys. Rev. Lett.* **110** 113601

[24] Hu Z D, Liang X, Wang J and Zhang Y 2016 *Opt. Exp.* **24** 10817

[25] Domenikou N, Iliopoulos N, Terzis A F, Yannopapas V and Paspalakis E 2019 *Quantum Inf. Proc.* **18** 362

[26] Tang W, Lin F, Zhu X and Fang Z 2019 *Phys. Rev. B* **100** 165415

[27] Ryom J, Ko M, Kim N, Choe S, Kim C and Kim S 2021 *Plasmonics* **16** 1577

[28] Li Y and Argyopoulos 2021 *Appl. Phys. Lett.* **119** 211104

[29] Ryom J, Kim N, Ko M and Choe S 2022 *Plasmonics* **17** 949

[30] Zayats A V, Smolyaninov I I and Maradudin A A 2005 *Phys. Rep.* **408** 131

[31] Martin-Cano D, González-Tudela A, Martín-Moreno L, García-Vidal F J, Tejedor C and Moreno E 2011 *Phys. Rev. B* **84** 235306

[32] Xu S and Fan S 2019 *Phys. Rev. A* **99** 063806

[33] Boroviks S, Lin Z H, Zenin V A, Ziegler M, Dellith A, Gonçalves P A D, Wolff C, Bozhevolnyi S I, Huang J S and Mortensen N A 2022 *Nat. Commun.* **13** 3105

[34] Huang Y, Zheng J, Pan B, Song L, Chen K A, Yu Z, Y H and Dai D 2022 *APL Photonics* **7** 051301

[35] Saeed M, Ghaffar A, Rehman S U, Naz M Y, Shukrullah S and Naqvi Q A 2022 *Plasmonics* **17** 901

[36] Yang L, Li P, Wang H and Li Z 2018 *Chin. Phys. B* **27** 094216

[37] Smith C L C, Stenger N, Kristensen A, Mortensenb N A and Bozhevolnyid S I 2015 *Nanoscale* **7** 9355

[38] Ficek Z and Tanaś R 2002 *Phys. Rep.* **372** 369

[39] Dzsotjan D, Sorensen A S and Fleischhauer M 2010 *Phys. Rev. B* **82** 075427

[40] Martin-Cano D, Martin-Moreno L, Garcia-Vidal F J and Moreno E 2010 *Nano Lett.* **10** 3129

[41] Jones S J, Wiseman H M and Doherty A C 2007 *Phys. Rev. A* **76** 052116

[42] Vandenberghe L and Boyd S 1996 *SIAM Rev.* **38** 49

[43] Skrzypczyk P, Navascués M and Cavalcanti D 2014 *Phys. Rev. Lett.* **112** 180404

[44] Wootters W K 1998 *Phys. Rev. Lett.* **80** 2245

[45] Ollivier H and Zurek W H 2001 *Phys. Rev. Lett.* **88** 017901

[46] Baumgratz T, Cramer M and Plenio M B 2014 *Phys. Rev. Lett.* **113** 140401

[47] Chen L and Zhang Y Q 2017 *Europhys. Lett.* **120** 60007

[48] Zhang Y Q and Sun Y T 2019 *Quantum Inf. Process.* **18** 1

[49] Yu T and Eberly J H 2009 *Science* **323** 598

[50] Uola R, Costa A C S, Nguyen H C and Gühne O 2020 *Rev. Mod. Phys.* **92** 015001